Heteroatom Chemistry
Volume 5, Number 5/6, 1994

Ab Initio Study of Ion-Molecule Reactions between $H_2SiNH_2^+$ and NH_3

Susumu Kawauchi*

Information and Systems Department, Showa Denko K.K., 1-13-9 Shiba Daimon, Minato-ku, Tokyo 105, Japan

Akitomo Tachibana** and Tokio Yamabe[a]

Division of Molecular Engineering, Faculty of Engineering, Kyoto University, Kyoto 606-01, Japan

[a]*Institute for Fundamental Chemistry, 34-4 Nishihiraki-cho, Takano, Sakyo-ku, Kyoto 606, Japan*

Received 15 March 1994; revised 8 September 1994

ABSTRACT

Ion-molecule reaction pathways between $H_2SiNH_2^+$ and NH_3 have been examined by ab initio quantum chemical techniques using polarized split-valence basis sets and including the effects of electron correlation and zero-point energy corrections. The proton transfer (PT), hydrogen abstraction (HA), electron transfer (ET), and hydride transfer (HT) processes are thermodynamically unfavorable. The eliminative addition (EA) processes, in spite of their exothermicities, are also unfavorable, because they have activation barriers. The ammonia exchange (AE) process is most likely to occur among the reactions between $H_2SiNH_2^+$ and NH_3 without an activation barrier. Therefore, $H_2SiNH_2^+$ indicates apparent unreactivity toward NH_3. This agrees well with the experimental result reported by Haller that SiH_4N^+ apparently does not react with NH_3.

INTRODUCTION

In a preceding article, we investigated the ion-molecule reactions between SiH_3^+ and NH_3 theoretically for understanding the chemical reaction mechanisms in the plasma-enhanced chemical vapor deposition (PECVD) of silicon nitride [1]. It was predicted that eliminative addition (EA) and proton transfer (PT) are dominant processes, but hydrogen abstraction (HA), electron transfer (ET), and hydride transfer (HT) are negligible. This is in good agreement with recent experimental results reported by Haller [2] that EA and PT are the primary channels observed in the reactions between SiH_3^+ and NH_3. In addition, we suggested that $HSiNH_3^+$ and $H_2SiNH_2^+$ may be observed independently as the EA products, because the isomerization needs a large activation energy of 55.0 kcal mol^{-1} [1].

It is interesting to clarify the contribution of $HSiNH_3^+$ and $H_2SiNH_2^+$ whether further Si–N bond propagation in the PECVD is possible. However, Haller reported that the EA product ions, SiH_xN^+ (x = 2–4), are unreactive toward silane and ammonia. He therefore concluded that an ionic chain propagation reaction is not responsible for Si–N bond formation in the mixed silane-ammonia plasma.

The purpose of the present work is to clarify such unreactivity of $H_2SiNH_2^+$ toward NH_3 theo-

Dedicated to Prof. Adrian Gibbs Brook on the occasion of his seventieth birthday.

*Present address: Department of Polymer Science, Tokyo Institute of Technology, Ookayama, Meguro-ku, Tokyo 152, Japan.

**To whom correspondence should be addressed.

1042-7163/94/$5.00 + .25

retically. According to our preceding study of the reactions between SiH_3^+ and NH_3 [1], we have investigated the following six possible reactions including ammonia exchange (AE) by using ab initio quantum chemical techniques:

$$\text{EA: } H_2SiNH_2^+ + NH_3 \rightarrow SiN_2H_5^+ + H_2 \quad (1)$$

$$\text{PT: } H_2SiNH_2^+ + NH_3 \rightarrow SiNH_3 + NH_4^+ \quad (2)$$

$$\text{ET: } H_2SiNH_2^+ + NH_3 \rightarrow H_2SiNH_2 + NH_3^+ \quad (3)$$

$$\text{HA: } H_2SiNH_2^+ + NH_3 \rightarrow H_3SiNH_2^+ + NH_2 \quad (4)$$

$$\text{HT: } H_2SiNH_2^+ + NH_3 \rightarrow H_3SiNH_2 + NH_2^+ \quad (5)$$

$$\text{AE: } H_2SiNH_2^+ + NH_3 \rightarrow NH_3 + H_2SiNH_2^+ \quad (6)$$

A further study of the reactions of $HSiNH_3^+$ with NH_3, as well as the reactions of $H_2SiNH_2^+$ and $HSiNH_3^+$ with SiH_4, will be presented in a subsequent article.

METHODS OF CALCULATION

Molecular orbital calculations were performed with the GAUSSIAN 92 program [3]. The geometries were optimized by the analytical energy gradient method of the Hartree–Fock theory by using the polarized split-valence 6-31G* basis set (denoted as HF/6-31G*) [4]. The optimized geometries are displayed in Figure 1. Theoretical harmonic vibrational frequencies were obtained from analytical second derivatives to verify each equilibrium structure as a true energy minimum or a saddle point. Zero-point vibrational energies (ZPEs) were then scaled by a factor of 0.89 [4]. To obtain reliable energetics, single-point energy calculations were carried out at the second-order and third-order Møller–Plesset perturbation theories [4], and at the single- and double-substituted configuration interaction (CISD) [5] including unlinked cluster quadruple corrections (QC) [6], by using the 6-31G** basis set (denoted as MP2/6-31G**, MP3/6-31G**, and CISD + QC/6-31G**, respectively). The calculated total energies and ZPEs are listed in Table 1. The relative energies for $H_2SiNH_2^+$ and NH_3 were obtained (see Table 2).

RESULTS AND DISCUSSION

$H_3NSiNH_2^+$ and $H_2NSiHNH_2^+$ are obtained as equilibrium structures of the EA product $SiN_2H_5^+$. Figures 1c and 1e show the HF/6-31G* optimized geometries. $H_3NSiNH_2^+$ has a C_s structure with two Si–N bonds whose lengths of 1.675 and 2.035 Å are comparable to that of 1.706 Å in $HSiNH_2$ and that of 2.012 Å in $HSiNH_3^+$ [1], respectively. On the other hand, $H_2NSiHNH_2^+$ has a C_{2v} structure with two equivalent Si–N bonds, whose length of 1.640 Å is comparable to that of 1.634 Å in $H_2SiNH_2^+$ [1]. Therefore, $H_3NSiNH_2^+$ and $H_2NSiHNH_2^+$ correspond to a substituted silylene and a substituted silyl cation, respectively. $H_2NSiHNH_2^+$ is 3.3 kcal mol^{-1} more stable than $H_3NSiNH_2^+$ at the CISD + QC/6-31G** level.

The PT product $SiNH_3$ has two equilibrium structures, $HSiNH_2$ and H_2SiNH. They both have C_s planar structures, whose Si–N bond lengths are 1.706 and 1.573 Å, respectively. $HSiNH_2$ is 17.8 kcal mol^{-1} more stable than H_2SiNH at the CISD + QC/6-31G** level (Table 2). These are in excellent agreement with the previous result reported by Truong and Gordon [7] that the HF/6-31G** bond lengths are 1.708 and 1.576 Å, respectively, and the energy difference calculated at MP4/6-311G** is 17.9 kcal mol^{-1}.

The ET product H_2SiNH_2 has a C_s bending structure (Figure 1l), whose SiN bond length of 1.729 Å is distinctly longer than that of 1.634 Å in $H_2SiNH_2^+$. An electron attached to $H_2SiNH_2^+$ leads to H_2SiNH_2. As shown in Table 2, the adiabatic electron affinity of $H_2SiNH_2^+$ is 6.27 eV at the CISD + QC/6-31G** level. Thus, $H_2SiNH_2^+$ can act as an electron acceptor to form the CT complex with NH_3 similar to SiH_3^+. This will be discussed later.

The HA product $H_3SiNH_2^+$ was optimized as a C_s structure in Figure 1(m). $H_3SiNH_2^+$ has a small imaginary frequency of $26i$ cm^{-1}, which corresponds to internal rotation. We have failed in removing the imaginary frequency because of the very flat nature of the potential energy surface of $H_3SiNH_2^+$. $H_3SiNH_2^+$ has the longer SiN single bond of 1.913 Å than that of 1.724 Å in H_3SiNH_2. This means that an electron detachment causes the internal rotation barrier to be lower, because the SiN bond is weakened. Table 2 shows that $H_3SiNH_2^+$ is 204.4 kcal mol^{-1} (8.87 eV) higher in energy than H_3SiNH_2 at the CISD + QC/6-31G** level. This energy difference corresponds to the adiabatic ionization potential of H_3SiNH_2.

The relative energies for the reactions between $H_2SiNH_2^+$ and NH_3 in Table 2 are not sensitive to the basis set but are sensitive to the correlation effects. This is similar to the situation of the reactions between SiH_3^+ and NH_3 [1]. In particular, the correlation effects are quite large for the ET, HA, and HT processes. Since the ET, HA, and HT processes have high endothermicities at any levels of calculations (73.6, 72.4, and 145.1 kcal mol^{-1}, respectively, at the CISD + QC/6-31G** level), they are negligible under thermodynamic considerations. The PT processes have relatively small endothermicities (2.1 and 19.9 kcal mol^{-1}). The PT processes may also be negligible. These are in accord with Haller's experimental result for the reaction between SiH_4N^+ and NH_3 that the ET, HA, HT, and PT processes were not detected [2]. On the other hand, the EA processes have exothermicities of 25.3 and 28.6 kcal mol^{-1}.

Thus, in order to completely interpret the unreactivity of $H_2SiNH_2^+$ toward NH_3, the detailed re-

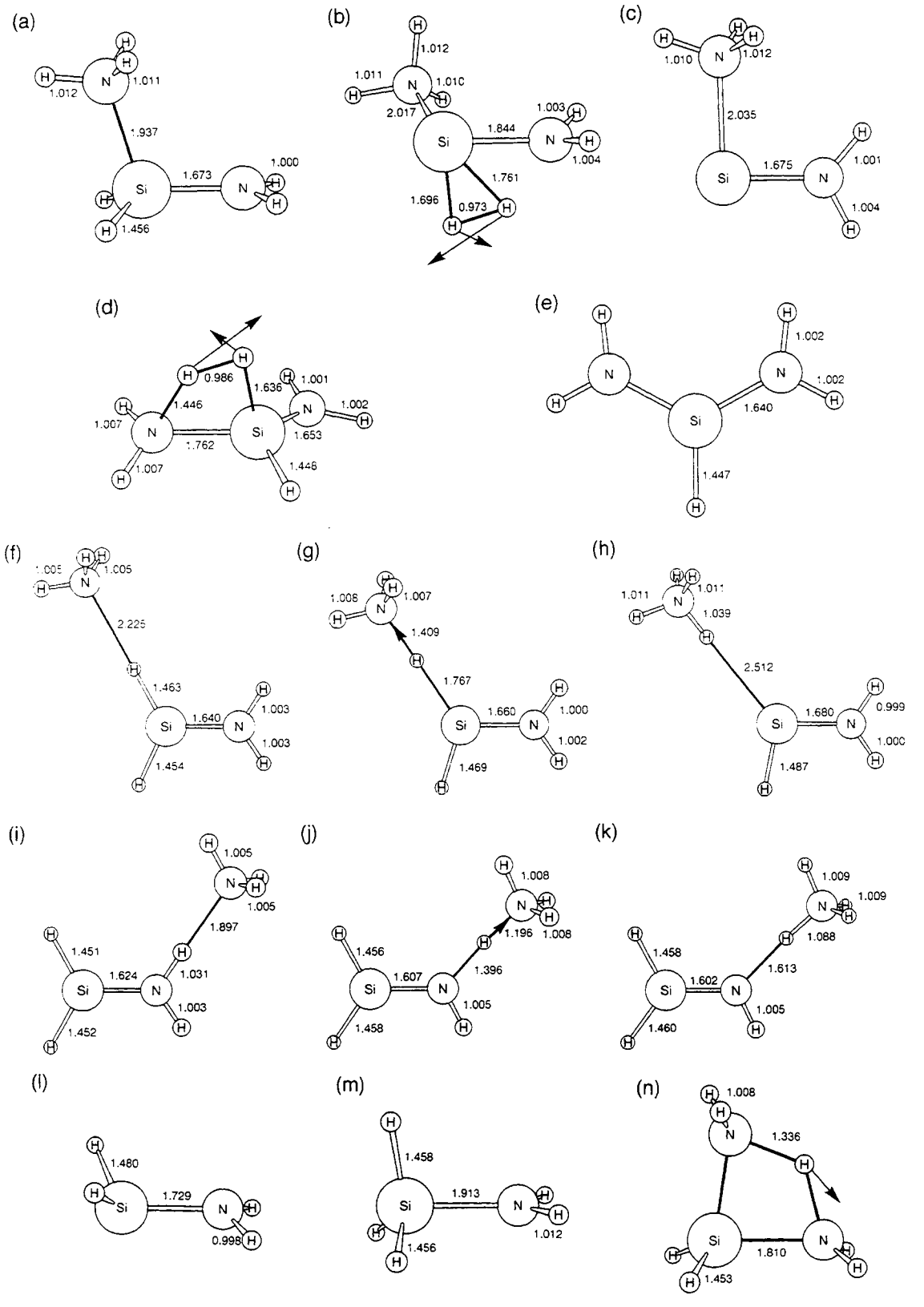

FIGURE 1 HF/6-31G* optimized structures: (a) $(H_3N \cdot SiH_2NH_2)^+$ (C_s), (b) TS1 (C_1), (c) $H_3NSiNH_2^+$ (C_s), (d) TS2 (C_1), (e) $H_2NSiHNH_2^+$ (C_{2v}), (f) $(H_3N \cdot HSiHNH_2)^+$ (C_s), (g) TS3 (C_s), (h) $(H_3NH \cdot SiHNH_2)^+$ (C_s), (i) $(H_3N \cdot HNHSiH_2)^+$ (C_1), (j) TS4 (C_1), (k) $(H_3NH \cdot NHSiH_2)^+$ (C_1), (l) H_2SiNH_2 (C_s), (m) $H_3SiNH_2^+$ (C_s), and (n) TS5 (C_{2v}). Bond lengths are in angstroms. Arrows in transition state structures show the eigenvector associated with the imaginary frequency.

TABLE 1 Total Energies and Zero-Point Energies (ZPEs)[a]

Species	*HF/6-31G**	*HF/6-31G***	*MP2/6-31G***	*MP3/6-31G***	*CISD + QC/6-31G***	*ZPE*
H_2[b]	−1.12683	−1.13133	−1.15765	−1.16314	−1.16511	5.91
NH_2^-[b]	−55.12729	−55.13507	−55.25788	−55.27755	−55.28662	11.00
NH_2[b]	−55.55770	−55.56482	−55.70971	−55.72540	−55.72914	11.49
NH_3^+[b]	−55.87324	−55.88489	−56.02863	−56.04517	−56.04922	19.55
NH_3[b]	−56.18436	−56.19553	−56.38295	−56.39576	−56.39870	20.67
NH_4^+[b]	−56.53077	−56.54552	−56.73340	−56.74790	−56.75101	29.76
$HSiNH_2$	−345.08768	−345.09701	−345.35355	−345.37383	−345.38181	20.07
H_2SiNH	−345.05117	−345.05877	−345.32739	−345.34023	−345.34991	17.78
$H_2SiNH_2^-$[b]	−345.43914	−345.45085	−345.70552	−345.72494	−345.73230	25.88
H_2SiNH_2	−345.66304	−345.67413	−345.93146	−345.95303	−345.96024	24.33
$H_3SiNH_2^-$	−345.99361	−346.00561	−346.23786	−346.26883	−346.27768	29.49
H_3SiNH_2	−346.28394	−346.29647	−346.57244	−346.59745	−346.60443	30.09
$H_3NSiNH_2^+$	−400.52153	−400.54000	−400.96919	−400.99665	−401.00447	39.59
$H_2NSiHNH_2^+$	−400.53378	−400.55236	−400.97541	−400.99885	−401.00593	37.19
$(H_3N \cdot SiH_2NH_2)^+$	−401.71702	−401.73904	−402.18484	−402.21638	−402.22397	50.31
$(H_3N \cdot HSiHNH_2)^+$	−401.64165	−401.66456	−402.10964	−402.14134	−402.14990	47.88
$(H_3NH \cdot SiHNH_2)^+$	−401.64615	−401.67054	−402.11834	−402.15164	−402.15990	51.15
$(H_3N \cdot HNHSiH_2)^+$	−401.65258	−401.67509	−402.12401	−402.15460	−402.16332	48.51
$(H_3NH \cdot NHSiH_2)^+$	−401.63524	−401.65834	−402.11729	−402.14410	−402.15370	48.48
TS1	−401.56779	−401.59790	−402.06455	−402.09656	−402.10488	48.16
TS2	−401.59328	−401.62346	−402.08546	−402.11335	−402.12133	46.13
TS3	−401.62729	−401.65149	−402.10677	−402.13706	−402.14542	47.23
TS4	−401.63440	−401.65858	−402.11936	−402.14593	−402.15530	46.35
TS5	−401.65482	−401.67988	−402.14026	−402.16834	−402.17637	47.68

[a]At the HF/6-31G* optimized geometries; total energies in au and ZPEs in kcal mol^{-1}. ZPEs were scaled by 0.89.
[b]Data are taken from Ref. [1].

action pathways for the EA, PT, and AE processes are examined:

$$H_2SiNH_2^+ + NH_3 \rightarrow (H_3N \cdot SiH_2NH_2)^+ \rightarrow TS1 \rightarrow H_3NSiNH_2^+ + H_2 \quad (7)$$

$$H_2SiNH_2^- + NH_3 \rightarrow (H_3N \cdot SiH_2NH_2)^+ \rightarrow TS2 \rightarrow H_2NSiHNH_2^+ + H_2 \quad (8)$$

$$H_2SiNH_2^+ + NH_3 \rightarrow (H_3N \cdot HSiHNH_2)^+ \rightarrow TS3 \rightarrow (H_3NH \cdot SiHNH_2)^+ \rightarrow HSiNH_2 + NH_4^+ \quad (9)$$

$$H_2SiNH_2^+ + NH_3 \rightarrow (H_3N \cdot HNHSiH_2)^+ \rightarrow TS4 \rightarrow (H_3NH \cdot NHSiH_2)^+ \rightarrow H_2SiNH + NH_4^+ \quad (10)$$

$$H_2SiNH_2^+ + NH_3 \rightarrow (H_3N \cdot SiH_2NH_2)^+ \rightarrow TS5 \rightarrow (H_2NSiH_2 \cdot NH_3)^+ \rightarrow NH_3 + H_2NSiH_2^+ \quad (11)$$

For the EA and AE processes, reactions 7, 8, and 11, the interaction of Si of $H_2SiNH_2^+$ with NH_3 initially leads to an ion-molecule complex $(H_3N \cdot SiH_2NH_2)^+$. The optimized structure is displayed in Figure 1(a). The $(H_3N \cdot SiH_2NH_2)^+$ complex has the high interaction energy of −54.6 kcal mol^{-1} at the CISD + QC/6-31G** level. Analogous to $(H_3Si \cdot NH_3)^-$ [1], which is an ion-molecule complex between SiH_3^- and NH_3, the high complexation energy of $(H_3N \cdot SiH_2NH_2)^+$ is ascribed to a charge-transfer interaction between the LUMO of $H_2SiNH_2^+$ and the HOMO of NH_3. $H_2SiNH_2^+$ can act as an electron acceptor, as discussed above, and NH_3 as an electron donor. It is worthwhile to note here that the complexation energy of $(H_3N \cdot SiH_2NH_2)^+$ is smaller than that of $(H_3Si \cdot NH_3)^+$ (76.5 kcal mol^{-1} [1]); in addition, the transferred electron density of 0.319*e* from NH_3 to $H_2SiNH_2^+$ in the $(H_3N \cdot SiH_2NH_2)^+$ complex is smaller than that of 0.344*e* from NH_3 to SiH_3^+ in $(H_3Si \cdot NH_3)^+$ [1]. These results can be explained by the electron-donative effect of the NH_2 group as follows. Although the p-π orbital on silicon in $H_2SiNH_2^+$ seems formally empty because of its atomic charge on silicon (+1.015), 0.272*e* occupy the p orbital on silicon perpendicular to the molecular plane. This situation is quite different from SiH_3^+ in that the p orbital on silicon perpendicular to the SiH_3^+ plane is really empty. It is clear that $H_2SiNH_2^+$ is stabilized by back-donation from the electron lone-pair of NH_2 to the p-π orbital on silicon. This is further confirmed by the LUMO of $H_2SiNH_2^+$ (−4.60 eV) being higher in energy than that of SiH_3^+ (−6.67 eV). As a result, $H_2SiNH_2^+$ is a weaker electron acceptor than SiH_3^+.

TABLE 2 Relative Energies (kcal mol^{-1})[a]

Reactions	*HF/6-31G**	*HF/6-31G***	*MP2/6-31G***	*MP3/6-31G***	*CISD + QC/6-31G***
$H_2SiNH_2^+ + NH_3$	0	0	0	0	0
$\rightarrow H_3NSiNH_2^+ - H_2$	−16.64	−16.70	−25.12	−25.57	−25.25
$\rightarrow H_2NSiHNH_2^+ + H_2$	−26.74	−26.86	−31.43	−29.36	−28.58
$\rightarrow HSiNH_2 + NH_4^+$	6.45	5.69	4.23	2.63	2.14
$\rightarrow H_2SiNH + NH_4^+$	27.07	27.40	18.36	21.43	19.87
$\rightarrow H_2SiNH_2 + NH_3^+$	52.06	52.15	77.89	74.20	73.60
$\rightarrow H_3SiNH_2^+ - NH_2$	39.72	42.08	82.84	73.79	72.35
$\rightarrow H_3SiNH_2 + NH_2^+$	127.74	129.36	156.53	148.72	145.11
$\rightarrow (H_3N \cdot SiH_2NH_2)^+$	−54.93	−54.39	−56.71	−56.28	−54.58
$\rightarrow (H_3N \cdot HSiHNH_2)^+$	−10.06	−10.08	−11.96	−11.62	−10.53
$\rightarrow (H_3NH \cdot SiHNH_2)^+$	−9.62	−10.56	−14.15	−14.82	−13.54
$\rightarrow (H_3N \cdot HNHSiH_2)^+$	−16.29	−16.06	−20.35	−19.32	−18.32
$\rightarrow (H_3NH \cdot NHSiH_2)^+$	−5.44	−5.58	−16.16	−12.76	−12.32
→ TS1	36.57	32.03	16.62	16.76	18.00
→ TS2	18.54	13.96	1.46	4.19	5.64
→ TS3	−1.70	−2.53	−10.80	−9.59	−8.37
→ TS4	−7.04	−7.86	−19.59	−16.03	−15.45
→ TS5	−18.53	−19.89	−31.37	−28.77	−27.34
$H_2SiNH_2^+ + e$	0	0	0	0	0
$\rightarrow H_2SiNH_2$[b]	−142.05	−141.66	−143.33	−144.68	−144.58
	(−6.16)	(−6.14)	(−6.22)	(−6.27)	(−6.27)
H_3SiNH_2	0	0	0	0	0
$\rightarrow H_3SiNH_2^+ - e$[b]	181.58	181.91	209.34	205.60	204.43
	(7.87)	(7.89)	(9.08)	(8.92)	(8.87)

[a]Calculated using the HF/6-31G* optimized geometries. Energies including ZPE corrections.
[b]Data in parentheses are given in eV.

The transition states (TS1 and TS2) of the EA, Reactions 7 and 8, are shown in Figures 1b and 1d. The transition vectors, associated with imaginary frequencies of 1885*i* and 1787*i* cm^{-1}, correspond to the 1.1- and 1.2-H_2 eliminations from $(H_3N \cdot SiH_2NH_2)^+$, respectively. Table 2 indicates that Reactions 7 and 8 have barriers of 18.0 and 5.6 kcal mol^{-1}, respectively, at the CISD + QC/6-31G** level. Therefore, the EA processes are unfavorable. This is the reason why the EA is not detected experimentally [2]. However, the activation energy of Reaction 8 is relatively small. Although the reaction is too slow to be detected in the gas phase, it may contribute to surface reactions. Since Table 2 reveals that correlation effects are large for the activation barriers, more sophisticated methods, e.g., MP2(full)/6-31G* for geometry optimization, may have used to evaluate the barriers more accurately.

In order to predict further reactivity of the EA product $H_2NSiHNH_2^+$, the LUMO of $H_2NSiHNH_2^+$ is compared with that of $H_2SiNH_2^+$. The LUMO of $H_2NSiHNH_2^+$ (−2.68 eV) is higher in energy than that of $H_2SiNH_2^+$ (−4.60 eV). The p-π orbital on silicon in $H_2NSiHNH_2^+$ is occupied by 0.383*e*, which is larger than that in $H_2SiNH_2^+$. This leads to the prediction that $H_2NSiHNH_2^+$ will be less reactive toward NH_3 than $H_2SiNH_2^+$.

For the PT processes, Reactions 9 and 10, reactant complexes, $(H_3N \cdot HSiHNH_2)^+$ and $(H_3N \cdot HNHSiH_2)^+$, and product complexes, $(H_3NH \cdot SiHNH_2)^+$ and $(H_3NH \cdot NHSiH_2)^+$, were considered. The optimized structures are displayed in Figures 1f, 1i, 1h, and 1k, respectively. The transition states (TS3 and TS4) of the PT are shown in Figures 1g and 1j. Both the transition vectors, associated with imaginary frequencies of 1353*i* cm^{-1} and 940*i* cm^{-1}, correspond to the proton transfers. Table 2 shows that they do not have activation barriers (negative activation energies are −8.4 and −15.5 kcal mol^{-1}, respectively, at the CISD + QC/6-31G** level).

The transition state (TS5) of the AE, Reaction 11, is shown in Figure 1n. The transition vector, associated with an imaginary frequency of 1836*i* cm^{-1}, corresponds to the AE process. The AE is favorable because of its negative activation energy of −27.3 kcal mol^{-1} at the CISD + QC/6-31G** level, as shown in Table 2.

CONCLUSION

In this article, the reaction pathways between $H_2SiNH_2^+$ and NH_3 were studied theoretically in order to attempt to understand the apparent unreactivity of $H_2SiNH_2^+$ toward NH_3. Figure 2 sum-

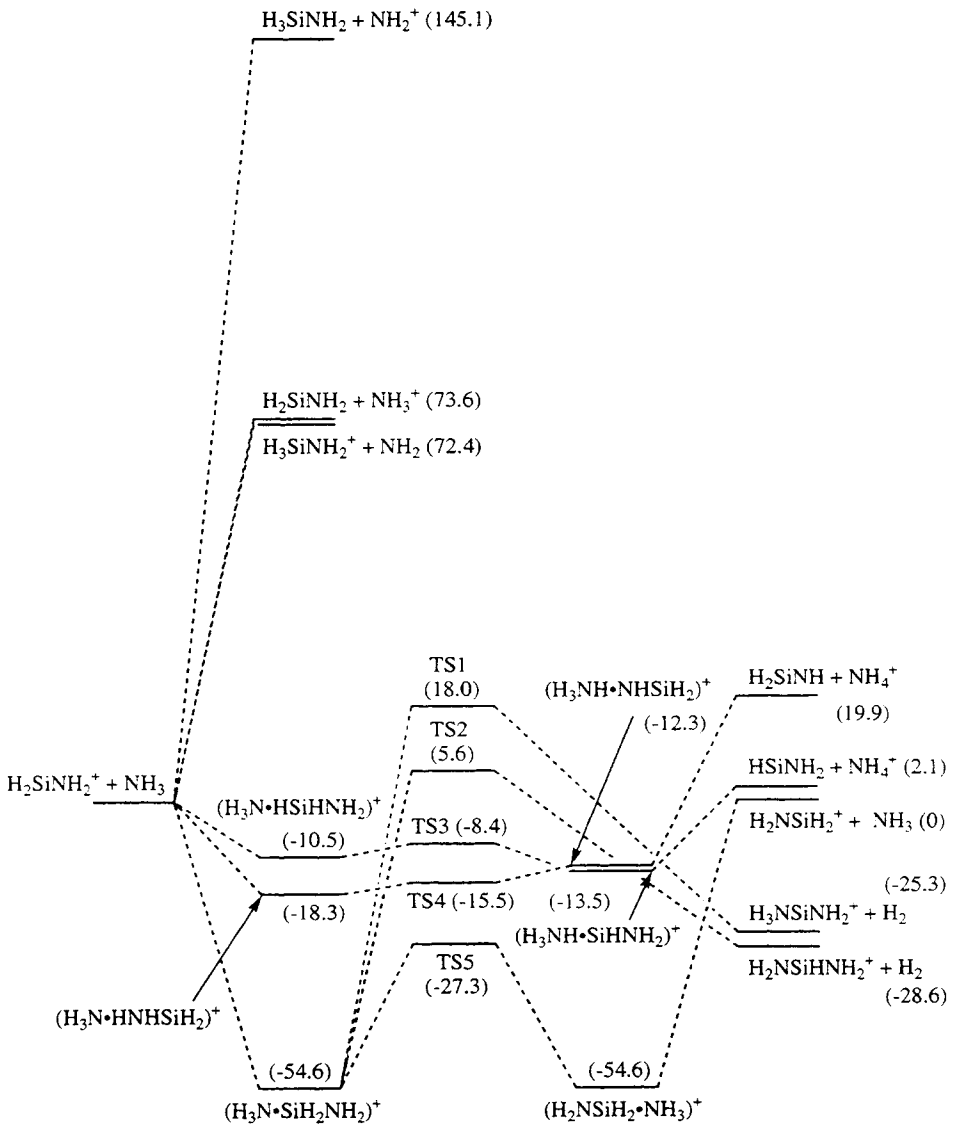

FIGURE 2 Energetics (kcal mol^{-1}) of ion-molecule reactions between $H_2SiNH_2^+$ and NH_3.

marizes the potential energy profile for the ion-molecule reaction between $H_2SiNH_2^+$ and NH_3 calculated at the CISD + QC/6-31G**//HF/6-31G* corrected with ZPEs.

The PT, HA, ET, and HT processes are thermodynamically unfavorable. The EA processes, in spite of their exothermicities, are also unfavorable, because they have activation barriers. The AE process is most likely to occur among the reactions between $H_2SiNH_2^+$ and NH_3, because the EA has no activation barrier. Therefore, $H_2SiNH_2^+$ indicates apparent unreactivity toward NH_3. This agrees well with the experimental result reported by Haller [2] that SiH_4N^+ apparently does not react with NH_3. This apparent unreactivity could be confirmed by a further experiment on the reaction between $H_2SiNH_2^+$ and ND_3 by using mass spectrometry. $H_2SiND_2^+$ should be found as a product.

Consequently, it seems that one can conclude that $H_2SiNH_2^+$ contributes little to further Si–N chain propagation in the PECVD of silicon nitride. However, it should be noted that, in the SiH_4-NH_3 plasma, $H_2SiNH_2^+$ is produced by the reactions between SiH_x^+ (x = 1–3) and NH_3 [2]. For example, the EA reaction between SiH_3^+ and NH_3 leading to $H_2SiNH_2^+$ is highly exothermic (42 kcal mol^{-1}) [1]. Therefore, taking into account the reactions leading to $H_2SiNH_2^+$, the EA process between $H_2SiNH_2^+$ and NH_3, as well as the PT, may occur and contribute to the Si–N chain propagation.

ACKNOWLEDGMENTS

This work was supported in part by a Grant-in-Aid for Scientific Research from the Ministry of Education, Science and Culture of Japan, for which the

authors express their gratitude. We wish to thank the Computer Center of the Institute for Molecular Science and the Data Processing Center of Kyoto University for their generous permission to use HITAC M-680 and S-820 and FACOM M-780/30, VP-400E, and VP-200 computers, respectively.

REFERENCES

[1] A. Tachibana, S. Kawauchi, N. Yoshida, T. Yamabe, K. Fukui, *J. Mol. Struct., 300*, 1993, 501.
[2] I. Haller, *J. Phys. Chem., 94*, 1990, 4135.
[3] M. J. Frisch, G. W. Trucks, M. Head-Gordon, P. M. W. Gill, M. W. Wong, J. B. Foresman, B. G. Johnson, H. B. Schlegel, M. A. Robb, E. S. Replogle, R. Gomperts, J. L. Andres, K. Raghavachari, J. S. Binkley, C. Gonzalez, R. L. Martin, D. J. Fox, D. J. DeFrees, J. Baker, J. J. P. Stewart, J. A. Pople: GAUSSIAN 92, Revision A, 1992. Gaussian Inc., Pittsburgh, PA.
[4] W. J. Hehre, L. Radom, P. R. Schlever, J. A. Pople: *Ab Initio Molecular Orbital Theory*, Wiley, New York, 1986.
[5] J. A. Pople, J. S. Binkley, R. Seeger, *Int. J. Quantum Chem. Symp., 10*, 1976, 1.
[6] S. R. Langhoff and E. R. Davidson, *Int. J. Quantum Chem., 8*, 1974, 61; E. R. Davidson, D. W. Silver, *Chem. Phys. Lett., 52*, 1978, 403.
[7] T. N. Truong, M. S. Gordon, *J. Am. Chem. Soc., 108*, 1986, 1775.